Spectrochimica Acta Part A: Molecular and Biomolecular Spectroscopy 204 (2018) 203–208

Contents lists available at ScienceDirect

Spectrochimica Acta Part A: Molecular and Biomolecular Spectroscopy

journal homepage: www.elsevier.com/locate/saa

Enhancement of local surface plasmon resonance (LSPR) effect by biocompatible metal clustering based on ZnO nanorods in Raman measurements

Sanghwa Lee [a], Seung Ho Lee [b], Bjorn Paulson [c,d], Jae-Chul Lee [e], Jun Ki Kim [a,d,*]

[a] Biomedical Engineering Research Center, Asan Medical Center, 88, Olympic-ro 43-gil, Songpa-gu, Seoul 05505, Republic of Korea
[b] Department of Biochemistry and Molecular Biology, College of Medicine, Kyung Hee University, 23, Kyungheedae-ro, Dongdaemun-gu, Seoul 02447, Republic of Korea
[c] Institute of Physics and Applied Physics, Yonsei University, 50 Yonsei-ro, Seodaemun-gu, Seoul 03772, Republic of Korea
[d] Department of Convergence Medicine, University of Ulsan College of Medicine, 88, Olympic-ro 43-gil, Songpa-gu, Seoul 05505, Republic of Korea
[e] Human Convergence Technology Group, Korea Institute of Industrial Technology, 143 Hanggaeul-ro, Sangrok-gu, Ansan, Kyeonggi-do 15588, Republic of Korea

ARTICLE INFO

Article history:
Received 22 February 2018
Received in revised form 1 June 2018
Accepted 12 June 2018
Available online xxxx

Keywords:
Surface-enhanced Raman spectroscopy
ZnO nanorods
Gold clustering
Finite element method (FEM)
Cell viability

ABSTRACT

The development of size-selective and non-destructive detection techniques for nanosized biomarkers has many reasons, including the study of living cells and diagnostic applications. We present an approach for Raman signal enhancement on biocompatible sensing chips based on surface enhancement Raman spectroscopy (SERS). A sensing chip was fabricated by forming a ZnO-based nanorod structure so that the Raman enhancement occurred at a gap of several tens to several hundred nanometers. The effect of coffee-ring formation was eliminated by introducing the porous ZnO nanorods for the bio-liquid sample. A peculiarity of this approach is that the gold sputtered on the ZnO nanorods initially grows at their heads forming clusters, as confirmed by secondary electron microscopy. This clustering was verified by finite element analysis to be the main factor for enhancement of local surface plasmon resonance (LSPR). This clustering property and the ability to adjust the size of the nanorods enabled the signal acquisition points to be refined using confocal based Raman spectroscopy, which could be applied directly to the sensor chip based on the optimization process in this experiment. It was demonstrated by using common cancer cell lines that cell growth was high on these gold-clad ZnO nanorod-based surface-enhanced Raman substrates. The porosity of the sensing chip, the improved structure for signal enhancement, and the cell assay make these gold-coated ZnO nanorods substrates promising biosensing chips with excellent potential for detecting nanometric biomarkers secreted by cells.

1. Introduction

Nanometer- and sub-micrometer-scale biological particles such as proteins, lipids, nucleic acids, exosomes, and metabolic contents have attracted much attention as biomarkers for the diagnosis of disease from biologically generated fluids such as blood, urine, and lymph. These biomarkers are now understood to be fundamental for healthy intercellular communication and are also generated in diseased cells. Label-free detection of these biomarkers can identify chemically distinct subpopulations arising from sorting choices during specific biogenesis and can also track post-translational modifications of biomarkers after their synthesis or release. Surface-enhanced Raman spectroscopy (SERS) is an approach to cellular analysis and identification that applies broad chemical spectroscopy to nanometer-sized biomarkers.

SERS is an attractive analytical and quantitative technique for label-free detection and identification of chemical and biological species [1, 2]. Following incident laser illumination at a single wavelength, Raman spectroscopy is able to identify biomarkers with a fingerprint of spectral peak positions, since the molecular vibrations of the sample are represented as a spectrum by inelastic scattering. Electromagnetic enhancement can be attained with this mechanism by using gold or silver nanoparticles, which cause the amplification of light by the local surface plasmon resonance (LSPR) effect [3, 4], in which a “hot spot” is formed on the surface of the SERS particles and the Raman signal is dramatically increased, enabling measurements on very small-sized samples. Recently, research even on the monomolecular scale has been made possible with the SERS technique [5–9]. According to finite element modeling analysis, a hot spot that gives a surface enhancement effect of about 108° is formed between gold colloids when the colloids have a diameter of 30 nm and are separated by a 2-nm gap [4]. In biomedical applications, biomarkers suitable for these nanogaps are extremely rare, and because of the size and shape of biological

* Corresponding author.
E-mail address: kim@amc.seoul.kr (J.K. Kim).

https://doi.org/10.1016/j.saa.2018.06.045
1386-1425/

molecules, research on SERS structure is required to optimize the LSPR effect.

Most attempts to improve SERS properties have focused on optimizing the surface of the substrate with the use of nanomaterials and nanostructures synthesized by sophisticated techniques, such as lithography patterning or high-temperature processes [7, 10–13]. Other research groups have deposited metal nanoparticles on paper [14–16] or applied a platform based on a silicon nanowire structure [17] to make a porous SERS substrate suitable for biological or liquid samples. Because of their amorphous nature, such papers, silicon nanowires, and epitaxially grown nanostructures are too dependent on the substrate and are difficult to combine with common cell culture substrates such as glass and Petri dishes. On the other hand, if a ZnO nanostructure-based platform is introduced, the substrate can be fabricated at a temperature of 100 °C or lower, and the SERS effect can be seen on amorphous substrates, such as glass and plastic, that are common in bioscience applications [18, 19]. In addition, it is possible to fabricate a nanostructure array without a lithographic process, and the manufacturing costs are significantly lower than those for other substrates, such as sapphire and Si wafers.

In the present study, SERS substrates based on a ZnO platform were fabricated, and gold nanoparticle ripening, which could not be performed on the ZnO-based SERS substrate [20], was performed by gold preferential growth and clustering on the ZnO nanorods to enhance the SERS effect. The length and density of the ZnO nanorods and the thickness of the deposited gold were modified to control the porosity and morphology of the gold nanostructure, and the mechanism of SERS enhancement was explained based on finite element analysis. Biocompatibility was evaluated to determine the presence or absence of toxicity for biological applications.

2. Material and Methods

2.1. Growth of ZnO Nanorods by the Hydrothermal Method

To prepare the ZnO-based SERS substrates, silicon wafers were scribed and broken into 2 × 2 cm pieces to grow the ZnO nanorods by the hydrothermal method [21]. The resulting chips were cleaned in acetone, methanol, and deionized water for 10 min each. A ZnO seed layer was deposited on the surface of the as-prepared samples using a sputtering system (SPS series, ULTECH). The sputtering process was carried out at a fixed working pressure of 6 mTorr with 100 W RF power under argon. Hydrothermal synthesis was utilized to grow vertically aligned ZnO nanorods. The ZnO growth solution was prepared by dissolving 0.015 M zinc nitrate hexahydrate ($Zn(NO_3)_2 \cdot 6H_2O$) (Sigma Aldrich) and hexamethylenetetramine (HMT) (Sigma Aldrich) in 200 mL of deionized water. A homogeneous aqueous solution was obtained by gentle stirring with a magnetic bar for 2 h at room temperature. The as-prepared samples were then immersed in the aqueous solution in an oven at 90 °C for 70 min. The experimental procedure, including measurement analysis, is shown schematically in Fig. 1.

2.2. Gold Deposition on ZnO Nanorods

After growth of the ZnO nanorods, the substrates were cleaned with deionized water and dried with nitrogen gas. Finally, the ZnO nanorods were coated with gold using an e-beam evaporator (EL-5, ULVAC). The thickness of the deposited gold was determined by measuring the thickness of a cross section of the target sample on a flat silicon wafer. The current, voltage and duration for deposition thicknesses of 100 and 200 nm were standardized. The morphology of the plane and cross-sectional nanorods was observed by field emission scanning electron microscopy (FESEM) (S-4700, Hitachi).

2.3. Cell Cultures

One breast cancer cell line, MDA-MB-231, was purchased from the Korean Cell Line Bank (Seoul, Korea). The cells were cultured in Dulbecco's modified Eagle's Minimal Essential Medium (DMEM) (Life Technologies, Grand Island, NY, USA) supplemented with 10% fetal bovine serum (FBS) (Hyclone Laboratories, Logan, UT, USA) and a 1% penicillin-streptomycin solution (Life Technologies) in a humidified 5% CO_2 incubator at 37 °C.

2.4. Cell Viability Assay

Cell viability analyses were based on MTT (3-(4,5-dimethylthiazol-2-yl)-2,5-diphenyl tetrazolium bromide) (Sigma Aldrich) assays. Cells

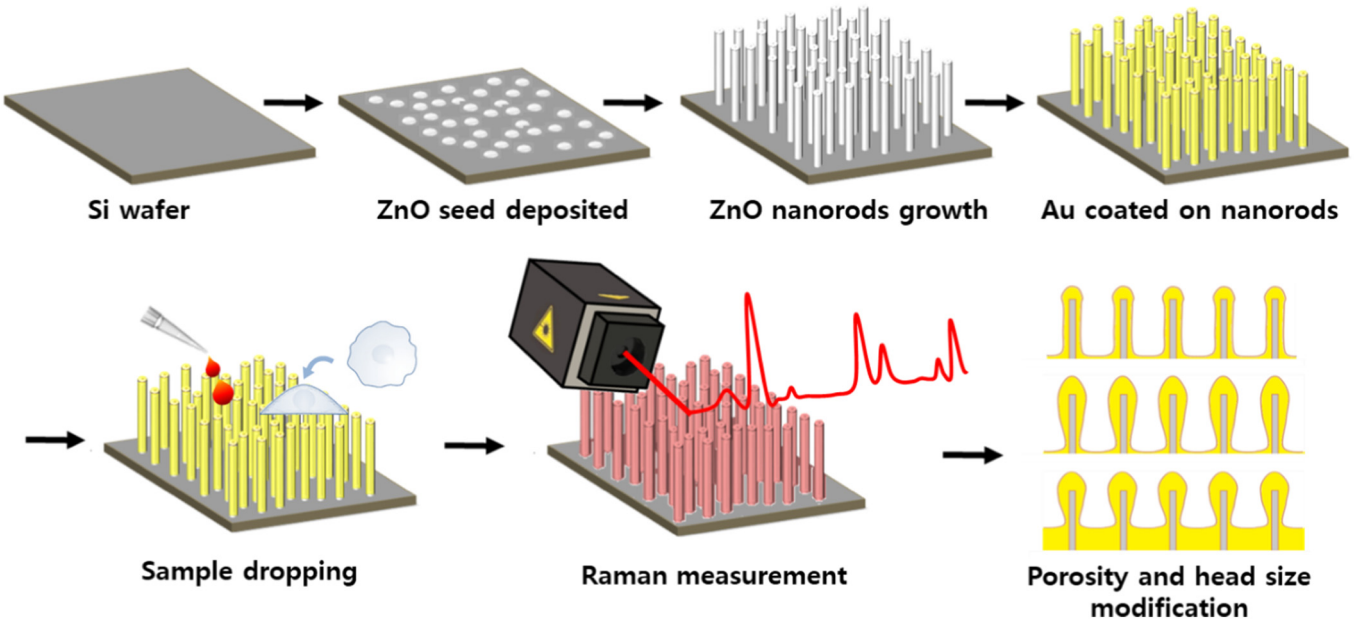

Fig. 1. Schematic of the experiment involving ZnO nanorods-based surface-enhanced Raman spectroscopy (SERS) substrate fabrication.

were plated at a density of 3×10^5 cells/well and incubated for 24 h. After deposition of ZnO, the cells were treated with 5 mg/mL MTT for 30 min and then dissolved using dimethyl sulfoxide (DMSO). The absorbance was measured at 540 nm with an ELISA microplate reader (Multiskan EX, Thermo Scientific, USA).

2.5. Raman Spectroscopy

Raman measurements (LabRam Aramis, Horiba) were carried out using a 785-nm diode laser in a confocal geometry with a 0.5 NA, ×50 objective lens and beam spot diameter ~1.9 μm. The spectrum of each point was measured in the range of 400 to 2500 cm^{-1} with a spectral resolution of 5 cm^{-1} and an integration time of 30 s at room temperature. After the Raman measurements, the spectrum was postprocessed by Savitzky-Golay smoothing, and a third-order polynomial fit to the auto-fluorescence background was subtracted. Rhodamine B (RhB) >95% purchased from Sigma Aldrich was used as a standard for Raman measurements.

2.6. Computational Analysis by FEM

The finite element method (FEM) was used with COMSOL Multiphysics software (COMSOL, USA) to simulate the SERS activities of the electromagnetic fields. Two-dimensional models for metallic-coated nanorod substrates with various metal sphere diameters were established. For a given boundary condition, the near-field distribution of the electromagnetic field was calculated to solve the time-harmonic Maxwell's equations at 785 nm excitation wavelength.

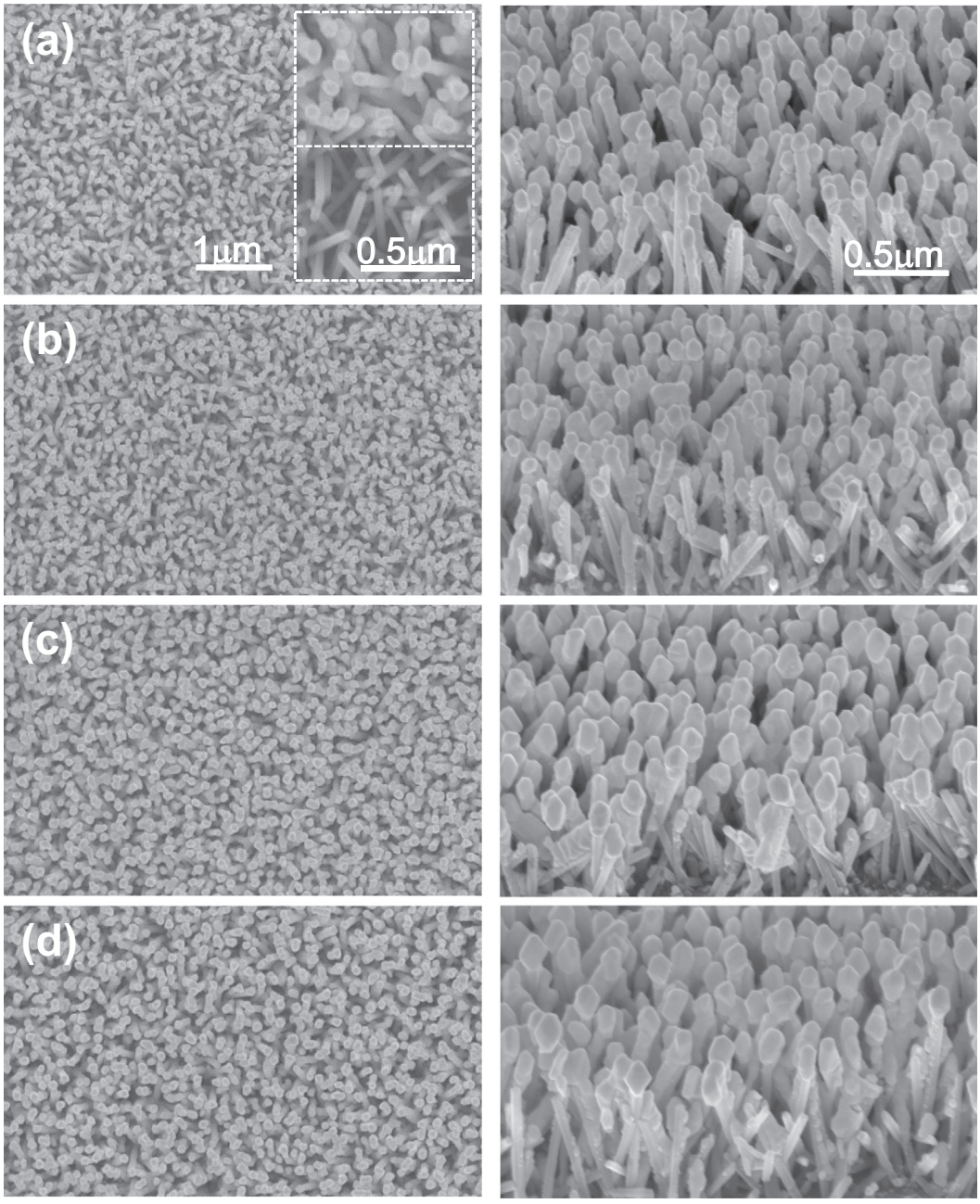

Fig. 2. Secondary electron images of the substrate with nanorod length and deposited gold thickness modified for (a) ZnO: 400 nm in length with 100 nm deposited gold, (b) ZnO: 600 nm in length with 100 nm gold, (c) ZnO: 400 nm in length with 200 nm deposited gold, and (d) ZnO: 600 nm in length with 200 nm deposited gold. The inset shows the initial difference in covering due to gold coating. (For interpretation of the references to colour in this figure legend, the reader is referred to the web version of this article.)

3. Results

3.1. Growth and Characterization of Gold-Coated ZnO Nanorods

In order to obtain a suitable porosity for the sample solution, the ZnO seed layer was modified and deposited such that the preferential growth direction of the ZnO nanorods was within about 10° from the vertical. An amount of gold with a height of 100 or 200 nm per unit area was deposited on nanorods with a length distribution of 300 to 450 or 500 to 650 nm, respectively. These four specimens were displayed with a secondary electron image of the plane and 45° tilt-view, as shown in Fig. 2. The top and bottom of the inset in Fig. 2 (a) show the substrates with gold deposited (top) and not deposited (bottom), and the ZnO is fully covered even when only 100 nm of gold is deposited. When gold deposition is increased to 200 nm, the thickness of the rods is about 10 to 30 nm greater than when gold deposition is not carried out. In addition, because the distribution of nanorod lengths has a standard deviation of 50 nm and the deposited gold is clustered at the ends of the rods, the distribution of the heights of the gold clusters undergoes a similar increase. Therefore, when the confocal Raman spectroscopic measurement is focused on the substrate surface, the Raman enhancement effect can be confirmed according to the head size.

3.2. Raman Enhancement and Reduction of Coffee-Ring Effects

To confirm the Raman enhancement effect of the SERS substrate based on ZnO nanorods, 10 μL of 1 mM RhB was dropped, and the signals were measured after natural drying. Fig. 3 (a) shows the enhancement of the Raman signal from 1000 to 1500 cm^{-1} according to each specimen. The greatest enhancement was observed for the 600-nm ZnO nanorods with 200 nm of deposited gold, which is a correction for the droplet area. When randomly measured on the sample surface, the 400-nm-long specimen, with the same average gold thickness, gave larger enhancements. Because the effective concentration and the LSPR enhancement characteristics differs between the two samples, a correction for the effective concentration is required as follows. The enhancement factor (EF) is calculated by the equation

$$\mathrm{EF} = \left(\frac{I_{SERS}}{I_{bare}}\right)\left(\frac{C_{bare}}{C_{SERS}}\right)$$

where C_{SERS} is the concentration of RhB on the gold-coated ZnO nanorod SERS substrate, I_{SERS} is the measured Raman intensity from the coated substrate, and C_{bare} and I_{bare} are the corresponding parameters for the bare substrate. The effective concentration of RhB at the beam spot in the dried samples varies across the sample, as the diffusion of the droplet depends upon the porosity of the specimen. In addition, even though samples with same volume are dropped in all experiments, the C_{bare}/C_{SERS} value is dependent on the correction for the area, since the droplet area is different for each sample after diffusing into the nanorods. Therefore, I_{SERS} enhancement due to substrate characteristics is largest in the 200-nm gold-coated nanorods 600 nm in length. This enhancement is the same for each specific peak, as shown in Fig. 3 (b). This measurement further demonstrates that the enhancement effect is compared without denaturation due to the strong electric field of the sample, as the relative ratio between peaks is not changed significantly.

The SERS substrates based on ZnO nanorods show no coffee-ring effect, as shown in Fig. 3 (c). Because of the rise in concentration at the edge of the region of deposition, the ring edges of RhB on bare substrates and of RhB on thin gold films show stronger Raman signals. On the other hand, nanorod substrates have larger values in the interior of the deposition ring.

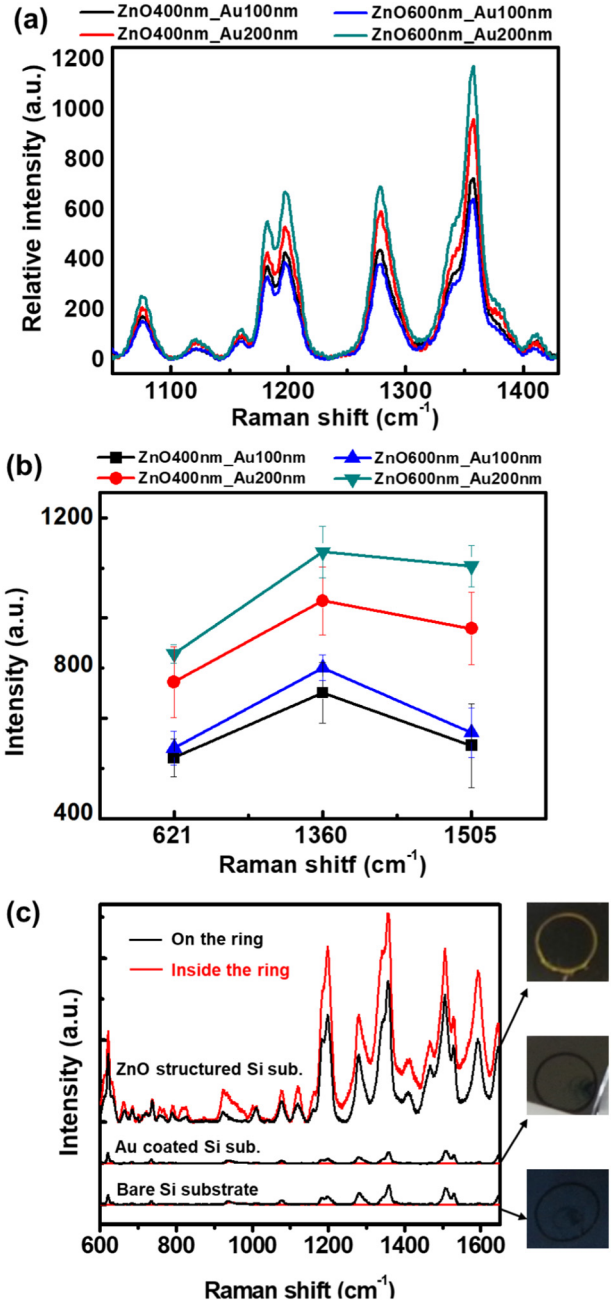

Fig. 3. (a) Raman signal enhancement of rhodamine B on each substrate. (b) Differences in the enhancement intensity of each specific peak according to the substrate. (c) Differences in the coffee-ring effect of the Raman signal depending on the nanorods.

3.3. Computational Analysis of ZnO-Based SERS Substrates

To understand the effect of gold cluster size on SERS enhancement, computational analysis using FEM was performed. Based on the data from secondary electron microscopy images, structures were modeled with 80-nm and 125-nm heads on nanorods 50 nm in width (including the gold coating) and 600 nm in length. Since Raman signal is enhanced by LSPR on a metal surface, the near-field distribution of the electric fields was calculated for a 785-nm incident light and parallel-plate boundary conditions with symmetry of the electric field. As shown in Fig. 4, there is almost no change in the full scale, regardless of the change in head width, and the electric field is distributed in the vertical direction of the rod. Comparing the sizes of these regions, the difference in area is about twice as much as the SERS intensity is twice as large. The width of the cross section of incident light is 2 μm, and the density of

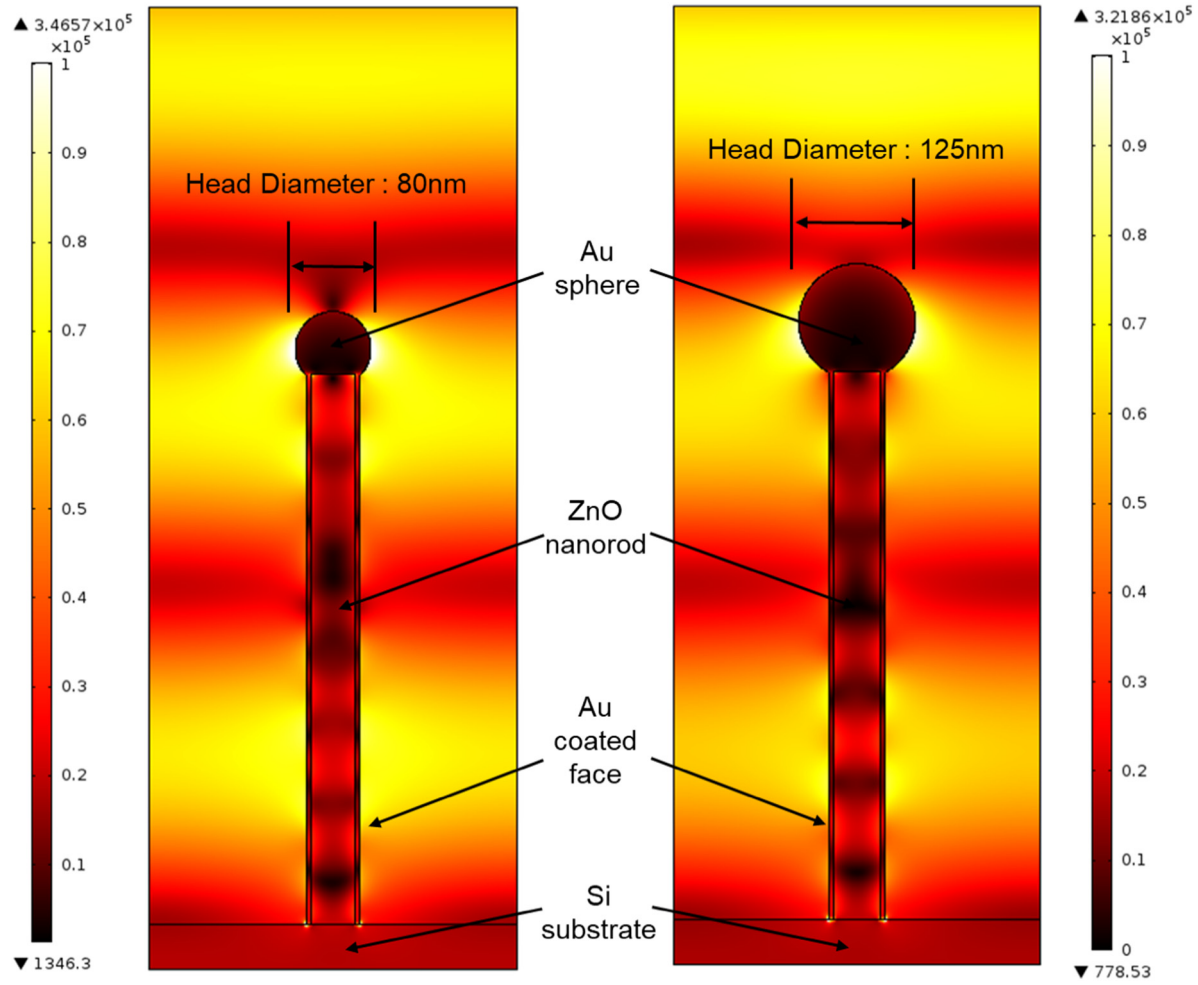

Fig. 4. Finite element analysis showing the difference in local surface plasmon resonance (LSPR) on ZnO nanorod-based SERS substrates with gold head diameters of 80 and 125 nm. (For interpretation of the references to colour in this figure legend, the reader is referred to the web version of this article.)

the nanorods within the region is constant, which suggests that the difference in SERS enhancement is caused by the increase in scatter contributing to inelastic scattering.

3.4. Toxicity of the SERS Substrate

Confirmation of biostability of the SERS substrate is required for Raman measurements of nanometer-sized biomarkers secreted by living cells. The toxic endogenous properties of gold nanoparticles have been reported previously [22], and ZnO nanorods are reported to be toxic to NIH 3T3 fibroblasts [23]. Therefore, assessment of toxicity needs to precede application to living cells. Fig. 5 shows the MTT assay results for the death of the breast cancer cell line MDA-MB-231 on the SERS substrate. The MDA-MB-231 line is frequently used in biotechnology applications, such as detecting cancer cell malignancy. Based on the results, the gold-clustered substrate of ZnO is suitable for experiments on the living breast cancer cell line.

4. Conclusions

We fabricated ZnO-nanostructured SERS substrates coated with gold nanoparticles and compared the differences in Raman effect surface enhancement by controlling the length of the nanorods and the volume of deposited gold. In secondary electron images, the nanorod heads were observed to increase in diameter much faster than diameter of the nanorods, when the amount of deposited gold was increased. As the volume of deposited gold increased, the signal also increased in proportion to the Raman signal enhancement according to the growth conditions of the substrate. Two-dimensional finite element analysis confirmed that the electric fields of nanorods with gold nanoclusters of 80 and 125 nm were distributed parallel to the substrate. When the size of the electric field was compared with a meaningful area, the corresponding area of the gold cluster was doubled as the amount of gold deposited increased from 100 nm to 200 nm per unit area, which became the basis for the increase in LSPR. In addition, the survival rate of the breast cancer cell line MDA-MB-231 on this substrate matched the

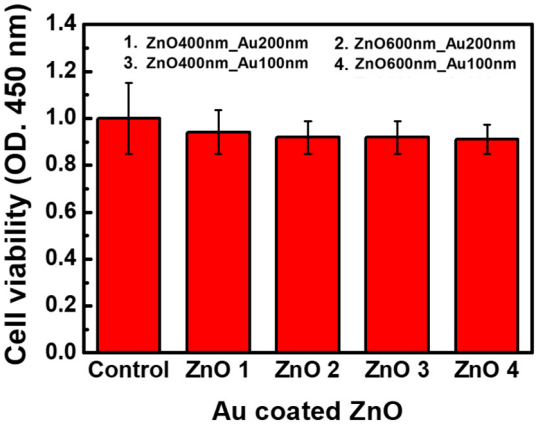

Fig. 5. Cell viability of MDA-MB-231 on each substrate by MTT assay.

survival rate on a control substrate. Therefore, the low-cost, gold-coated ZnO nanorods substrate may be used as a biosensing chip with excellent potential for detecting nanometric biomarkers secreted by the cells. The Raman-based sensing chip presented in this study was suitable for monitoring of living cells and utilized the phenomenon of gold clustering on the head of the nanorod in the signal optimization process for the measurement of biological samples. By acquiring a refined signal at the gold clusters in the confocal Raman setup, the ability to control porosity by controlling the length of the nanorods is also demonstrated. Furthermore, by fabricating SERS chips based on ZnO nanorods, it is possible to fabricate sensing chips at low temperatures on substrate materials used in biological research, such as glass and plastic.

Disclosures

The authors have no relevant financial interests in this article and no potential conflicts of interest to disclose.

Acknowledgements

This work was supported by the Basic Science Research Program (2014R1A1A2057773, 2015K2A7A1035896) through the National Research Foundation of Korea (NRF) funded by the Ministry of Science & ICT (MSIT), and by the Ministry of Trade, Industry & Energy (MOTIE) under Industrial Technology Innovation Program (10080726). This study was also supported by a grant (2015-641, 2015-646) from the Asan Institute for Life Sciences, Asan Medical Center, Seoul, Korea.

Declarations of interest

None.

References

[1] D. Cialla, et al., Surface-enhanced Raman spectroscopy (SERS): progress and trends, Anal. Bioanal. Chem. 403 (1) (2012) 27–54.
[2] S.W. Zeng, et al., Nanomaterials enhanced surface plasmon resonance for biological and chemical sensing applications, Chem. Soc. Rev. 43 (10) (2014) 3426–3452.
[3] P.L. Stiles, et al., Surface-enhanced Raman spectroscopy, Annu. Rev. Anal. Chem. 1 (2008) 601–626.
[4] P.G. Etchegoin, E.C. Le Ru, A perspective on single molecule SERS: current status and future challenges, Phys. Chem. Chem. Phys. 10 (40) (2008) 6079–6089.
[5] W.Y. Li, et al., Dimers of silver nanospheres: facile synthesis and their use as hot spots for surface-enhanced Raman scattering, Nano Lett. 9 (1) (2009) 485–490.
[6] Y.L. Wang, J. Irudayaraj, Surface-enhanced Raman spectroscopy at single-molecule scale and its implications in biology, Philos. Trans. R. Soc. B 368 (1611) (2013).
[7] J.D. Caldwell, et al., Large-area plasmonic hot-spot arrays: sub-2 nm interparticle separations with plasma-enhanced atomic layer deposition of Ag on periodic arrays of Si nanopillars, Opt. Express 19 (27) (2011) 26056–26064.
[8] S.J. Lee, A.R. Morrill, M. Moskovits, Hot spots in silver nanowire bundles for surface-enhanced Raman spectroscopy, J. Am. Chem. Soc. 128 (7) (2006) 2200–2201.
[9] S.L. Kleinman, et al., Creating, characterizing, and controlling chemistry with SERS hot spots, Phys. Chem. Chem. Phys. 15 (1) (2013) 21–36.
[10] N.A. Abu Hatab, J.M. Oran, M.J. Sepaniak, Surface-enhanced Raman spectroscopy substrates created via electron beam lithography and nanotransfer printing, ACS Nano 2 (2) (2008) 377–385.
[11] F. De Angelis, et al., Breaking the diffusion limit with super-hydrophobic delivery of molecules to plasmonic nanofocusing SERS structures, Nat. Photonics 5 (11) (2011) 683–688.
[12] N.A. Cinel, et al., E-beam lithography designed substrates for surface enhanced Raman spectroscopy, PhotonicS. Nanostruct. 15 (2015) 109–115.
[13] N.E. Marotta, et al., Patterned silver nanorod array substrates for surface-enhanced Raman scattering, Appl. Spectrosc. 63 (10) (2009) 1101–1106.
[14] Y.H. Ngo, et al., Paper surfaces functionalized by nanoparticles, Adv. Colloid Interf. Sci. 163 (1) (2011) 23–38.
[15] B.W. Li, et al., A fast and low-cost spray method for prototyping and depositing surface-enhanced Raman scattering arrays on microfluidic paper based device, Electrophoresis 34 (15) (2013) 2162–2168.
[16] W. Zhang, et al., Brushing, a simple way to fabricate SERS active paper substrates, Anal. Methods 6 (7) (2014) 2066–2071.
[17] M.S. Schmidt, J. Hubner, A. Boisen, Large area fabrication of leaning silicon nanopillars for surface enhanced Raman spectroscopy, Adv. Mater. 24 (10) (2012) Op11–Op18.
[18] B.A. Albiss, M.A. Al-Akhras, I. Obaidat, Ultraviolet photodetector based on ZnO nanorods grown on a flexible PDMS substrate, Int. J. Environ. Anal. Chem. 95 (4) (2015) 339–348.
[19] Y. Chen, et al., Ag nanoparticles-decorated ZnO nanorod array on a mechanical flexible substrate with enhanced optical and antimicrobial properties, Nanoscale Res. Lett. 10 (2015).
[20] G. Sinha, L.E. Depero, I. Alessandri, Recyclable SERS substrates based on au-coated ZnO nanorods, ACS Appl. Mater. Interfaces 3 (7) (2011) 2557–2563.
[21] Z.H. Ibupoto, et al., Hydrothermal growth of vertically aligned ZnO nanorods using a biocomposite seed layer of ZnO nanoparticles, Materials 6 (8) (2013) 3584–3597.
[22] W.H. De Jong, et al., Particle size-dependent organ distribution of gold nanoparticles after intravenous administration, Biomaterials 29 (12) (2008) 1912–1919.
[23] T.O. Okyay, et al., Antibacterial properties and mechanisms of toxicity of sonochemically grown ZnO nanorods, RSC Adv. 5 (4) (2015) 2568–2575.